

Received: 23.01.2025

Accepted: 04.05.2025

Research Article

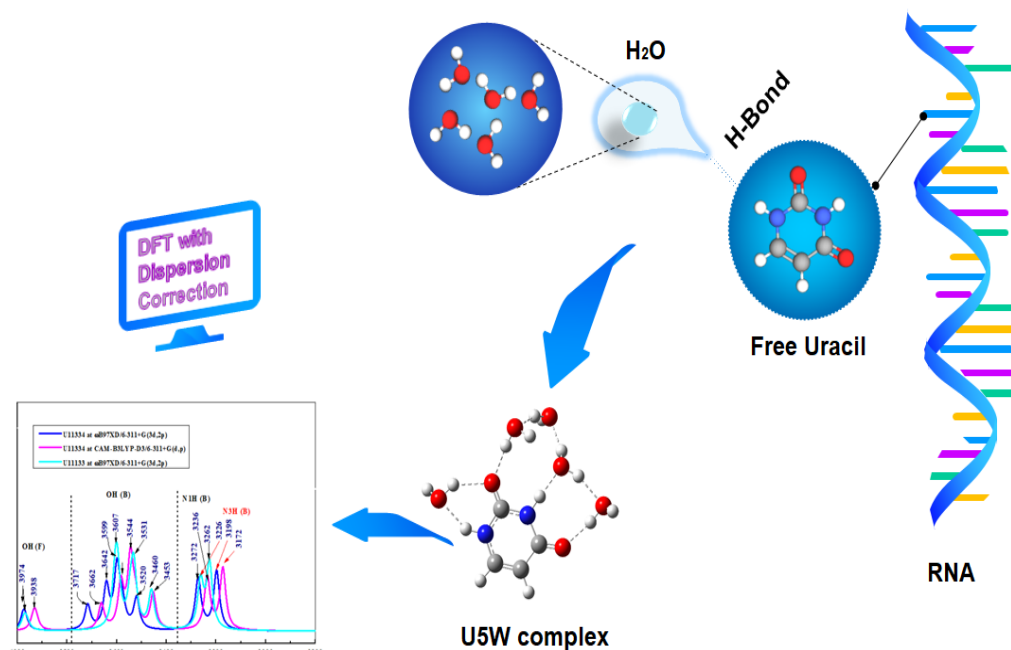
Dispersion-Corrected DFT Study of Uracil-5Water (U5W) Complexes: Energetic, Structures, Vibrational Properties, and Solvatochromic Shifts

Asma Hennouni^{a,1}, Mohammed El Amine Benmalti^a, Claude Pouchan^b, and Panagiotis Karamanis^b

^aLaboratoire de Structure Élaboration et Applications aux Matériaux Moléculaires (SEA2M), Chemin des crêtes (Ex INES), Université Abdelhamid Ibn Badis- Mostaganem, 27000, Algeria.

^bLaboratoire de Chimie Théorique et Physico-Chimie Moléculaire – UMR 5624, Fédération de recherche IPREM 2606, Université de Pau et Pays de l'Adour, IFR – Rue Jules Ferry, 64000 Pau, France.

Graphical abstract:



Abstract: Understanding uracil solvation is crucial for refining hydrogen bonding (H-bonding) models in aqueous systems, with implications for enzyme activity and drug design. In this study, we investigate novel uracil-5water (U5W) complexes, revealing an unusual H-bond arrangement that significantly influences vibrational properties. Density functional theory (DFT) calculations using ω B97XD and CAM-B3LYP-D3 functionals with various basis sets identified the most stable isomers (U11333, U11133, U12223), characterized by clustered water molecules and optimal H-bond lengths. New isomers (U11134, U11144, U11124) exhibited enhanced stability compared to previously reported configurations. Vibrational mode analysis confirmed hydration effects, notably influencing $\nu(\text{N-H})$ and $\nu(\text{C=O})$ shifts. The U12223 complex displayed a distinct $\text{N3H}\cdots\text{Ow}$ bond, altering vibrational behavior. These findings provide insights into H-bonding interactions and molecular stability, paving the way for future theoretical and experimental studies.

¹ Corresponding Authors

e-mail: asma.hennouni.etu@univ-mosta.dz

Keywords: Hydrogen bond, uracil-5water complexes, Density functional theory calculations, dispersion effect, infrared spectra.

1. Introduction

Uracil, a fundamental nucleobase in RNA, forms hydrogen bonds (H-bonds) via its C=O, N-H, and C-H groups, making it a valuable model for investigating hydration effects and nucleic acid stability. Water molecules play a crucial role in stabilizing these interactions by forming complex H-bond networks, which influence tautomeric equilibria, solvation dynamics, and biological function, with implications for drug design and biomolecular modeling [1–5]. Both experimental and theoretical studies have extensively examined uracil in isolated, hydrated, and solid-state environments [6–12]. Recent computational studies using M062X-based methods revealed that methimazole–uracil complexes exhibit partially covalent N–H···S bonds and significant charge transfer [11]. Investigations into the ionization energies of uracil–water clusters confirmed the coexistence of pure and mixed clusters stabilized by H-bonds [12]. Ultrafast decay processes in uracil excited states, dominated by C=C torsions, were elucidated through ADC(2) and surface hopping simulations [13–14]. Further studies employing DFT, MP2, and CCSD(T) methods analyzed monohydrated uracil complexes, providing detailed insights into interaction energies, electron distribution, and vibrational modes [15]. DFT-based investigations, particularly with B3LYP [16–18], highlighted the solute-induced constraints on water's H-bond network, with uracil–water interactions serving as a representative case. The energetic properties of uracil–water complexes have been widely investigated using ab initio methods, notably second-order MP2 [19,20]. Thicoipe et al. [21] applied B3LYP and B3LYP-D functionals to identify the most stable microhydrated nucleic acid base conformers, finding that dispersion effects become increasingly significant as the number of water molecules increases. However, B3LYP's limitations in describing long-range exchange interactions and dispersion effects have been documented [22,23]. To address this, CAM-B3LYP was developed with a long-range correction and D3 dispersion scheme, improving the accuracy of ΔE_{int} predictions [22]. Systematic errors in DFT energy calculations due

to electron density approximations can affect molecular geometries, especially in systems dominated by long-range interactions [24,25]. Scaling factors (SFs) are often applied to correct computed properties and improve predictive accuracy [26]. For neutral and anionic chromophores, TDDFT using CAM-B3LYP systematically underestimates two-photon absorption strengths relative to coupled-cluster values [27]. Grimme's D3 correction has improved the treatment of long-range intermolecular interactions and O–H vibrational modes in H-bonded systems, though it can adversely affect N–H stretching frequencies [26]. Experimental IR spectroscopy, combined with theoretical predictions, has advanced the understanding of vibrational frequencies in hydrated uracil systems [4,28–31]. Two new correction schemes involving scaling factors and empirical equations significantly reduced deviations compared to conventional single scaling factor approaches [32]. In studies of mixed sandwich complexes, CAM-B3LYP and ω B97XD tend to overestimate Rydberg transition energies, with discrepancies up to 2.3 eV compared to experiment [33]. Nevertheless, ω B97XD has demonstrated reliable performance in nucleobase, H-bonded, and aromatic systems [34–39], while CAM-B3LYP-D3 has yielded accurate benzene dimer interaction energies [40]. Both functionals approach CCSD(T) accuracy in many cases [22]. However, limitations in their description of specific interactions have been noted [34,41]. Despite progress, dispersion corrections in uracil–water clusters remain underexplored. Recent applications of VPT2 and molecular dynamics have improved predictions for hydrated uracil, with VPT2 offering better agreement with experimental data [42]. The superior accuracy of CAM-B3LYP-D3 and ω B97XD for spectroscopic properties has been confirmed in several studies [38,40,43]. The present work aims to identify the preferential hydration sites of water molecules on uracil, particularly via H-bonding to carbonyl and N–H groups, and to evaluate the relative stability of uracil–5water (U5W) complexes. Energetic, geometric, and vibrational properties are analyzed using dispersion-corrected DFT at the CAM-

B3LYP-D3/6-311+G(d,p), ω B97XD/6-311+G(3d,2p), and ω B97XD/aug-cc-pVTZ levels. Special focus is placed on H-bond lengths, vibrational scaling factors, and solvatochromic behavior. Moreover, a new class of U5W structures is proposed, distinct from the ring-like and cage-like configurations previously reported by Bachrach et al. [44].

2. Computational Method

In this study, DFT calculations were performed on the uracil-water complexes using the Gaussian16

program [45]. Two hybrid functionals, ω B97XD and CAM-B3LYP-D3, were employed. Structural optimizations and energetic properties of the complexes were calculated. We first started with the optimization of isolated uracil (Figure. 1) and water molecules followed by the calculation of the electronic energy (E_e).

The next step involved optimizing the U5W complexes by positioning the water molecule in four distinct regions, labeled 1, 2, 3, and 4, as shown in Figure. 1.

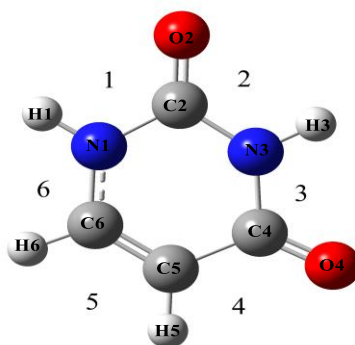


Figure 1. Isolated uracil with labeled sites of interactions.

To calculate the interaction energy using the Counterpoise (CP) method, the uncorrected interaction energy is first determined as follows:

$$\Delta E_{interaction}^{UnCP} = E_{AB} - (E_A + E_B) \quad (1)$$

where: E_{AB} is the total energy of the complex, E_A and E_B are the energies of the isolated fragments. However, due to Basis Set Superposition Error (BSSE), each fragment artificially stabilizes the other by borrowing basis functions, leading to an overestimated interaction energy. To correct for this, the CP method calculates the energy of each fragment in the basis set of the full complex:

ΔE_A^* =Energy of A in full basis set (with ghost orbitals)

ΔE_B^* =Energy of B in full basis set (with ghost orbitals)

The asterisk (*) represents monomers calculated with ghost orbitals, which account for basis set borrowing effects [48,49].

The BSSE correction is then given by:

$$BSSE = (E_A^* - E_A) + (E_B^* - E_B) \quad (2)$$

The corrected interaction energy is:

$$\Delta E_{int}^{CP} = \Delta E_{int}^{UnCP} - BSSE \quad (3)$$

equivalently : $\Delta E_{int}^{CP} = E_{AB} - (E_A + E_B) - BSSE$

By comparing the corrected and uncorrected interaction energies, the magnitude of BSSE can be analyzed to determine whether it is acceptable or significantly affecting the results. If the BSSE correction is small (e.g., < 1 kcal/mol), it may be negligible. However, if it is large, correction is necessary to ensure accurate interaction energy values.

The basis set superposition error (BSSE) was calculated using the CP correction method [46]. In this approach, each fragment is computed using the full basis set of the complex, ensuring that basis set borrowing effects are accounted for [47].

The relative interaction energy (ΔE_{intrel}) values for the various complexes are determined as the difference between the energy of each complex and that of the lowest energy complex. Quantitative analysis was performed using the dispersion-corrected ω B97XD functional, which combines the effective interaction of B97 [50] and Grimme's dispersion D2 [51] as utilized by Chai and Head-Gordon [52]. to create the range-separated hybrid

functional ω B97XD [52,53]. This analysis was conducted with both 6-311+G(3d,2p) and aug-cc-pVTZ basis sets. Additionally, the CAM-B3LYP-D3 Coulomb-attenuating method [54], which combines the B3LYP functional used by Becke [55], the three-parameter hybrid approach of Lee–Yang–Parr [56], and the long-range correction proposed by Tawada et al. [57], along with Grimme’s dispersion correction [23] (denoted as -D3), was applied with the 6-311+G(d,p) basis set. Frequency calculations were performed to confirm that the optimized structures correspond to true minima (i.e., no imaginary frequencies). The infrared absorption spectrum (IR) computed using the same level of theory.

Using both theoretically predicted (ω_i) and experimentally measured vibrational frequencies (ν_i), the SFs (c) were calculated according to the equation (2) obtained from the Computational Chemistry Comparison and Benchmark Database [58] to correct for anharmonicity effects.

We revealed the SFs of uracil and U5W complexes as shown in result section.

$$c = \frac{\sum(\nu_i \cdot \omega_i)}{\sum(\omega_i^2)} \quad (4)$$

The calculated spectra were then compared with experimental and previous data to identify characteristic H-bond and functional group vibrations.

The observed deviations were analyzed in terms of solvent effects, anharmonicity corrections, and basis set limitations. The agreement between theoretical and experimental results confirmed the reliability of the chosen computational methods.

The vibrational frequencies $\nu(\text{OH}(\text{F}))$, $\nu(\text{OH}(\text{B}))$, $\nu(\text{NH}(\text{F}))$, and $\nu(\text{NH}(\text{B}))$ of uracil and isomers of U5W in 3400-4000 cm^{-1} region and solvatochromic shift plotted using OriginPro 8.5 graphical software [59].

3. Results and discussion

3.1. Energetic properties

The interaction of five water molecules with uracil is considered a manageable number, allowing the study of significant solvation effects without imposing excessive computational demands. Which above this number, interactions between water and nucleic acid bases become significantly more complex. Therefore, it represents a balance between capturing sufficient interactions and maintaining computational feasibility,

corresponding to the first hydration shell commonly observed in biological systems. All initial configurations were fully optimized at the CAM-B3LYP-D3/6-311+G(d,p), ω B97XD/6-311+G(3d,2p), and ω B97XD/aug-cc-pVTZ levels of theory to obtain the final geometries, considering the basis set superposition error (BSSE) through CP correction [46], we determined the CP by calculating each fragment within the complex’s basis. Then, we calculated the frequency at the same level of theory. The most stable configurations were selected based on the lowest electronic ΔE_{int} , calculated as the difference between the energy of the U5W complex and the sum of the energies of uracil and five isolated water molecules.

The interaction of uracil with water occurs through H-bonds, where the N-H and C-H donor group or C=O acceptor group of uracil interacts with the oxygen acceptor atom or O-H donor group of water, as illustrated in Figure 1.

To identify the placement of water molecules at these sites, whether separately, together, or two water molecules at one site, we adopted a simplified abbreviation different to previous studies, which used letter-based labels [17,44]. The U5W complexes are denoted as UXXXXX, where U represents the uracil molecule and each X indicates the presence of a water molecule at a specific interaction site. The initial configurations presented in Figure 2 were constructed based on previous studies [17,21]. Additionally, Thicoipie [21] and Pouchan [42] identified new U5W complexes, namely U11223, U11113, and U11222.

The U11334 isomer is more stable than U11224, as it favors the formation of a water dimer at the third site rather than at the second site, as shown in Table 1. The stability is attributed to the shorter average N-H...O H-bond length of 1.779 Å. Additionally, U12234 exhibits greater stability due to the anti-positioning of the third water molecule, whereas in the U12334 isomer, this molecule adopts a syn-position. Our calculations using the ω B97XD functional with the 6-311+G(3d,2p) and aug-cc-pVTZ basis sets yielded the lowest MAE, at 0.8 and 3.8 kcal/mol, respectively (Table 1), indicating strong agreement with the reference B3LYP/DZP++ data [17]. The CAM-B3LYP-D3/6-311+G(d,p) method also showed reasonable agreement, with a MAE of 12.3 kcal/mol.

Asma Hennouni, Mohammed El Amine Benmalti, Claude Pouchan, and Panagiotis Karamanis

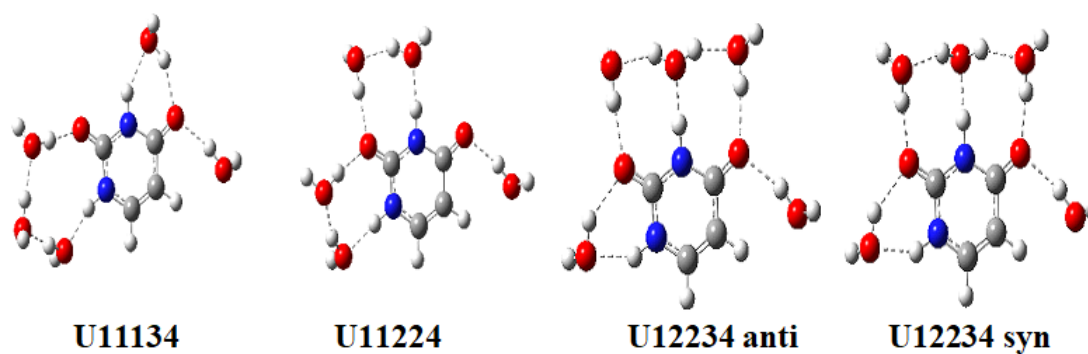


Figure 2. Representation of U5W interactions at CAM-B3LYP-D3/6-311+G(d,p), ω B97XD/6-311+G(3d,2p), and ω B97XD/aug-cc-pVTZ methods

Table 1. Interaction energy (ΔE_{int}) and relative interaction energy (ΔE_{intrel}) with both CP and UnCP of U5W complexes, expressed in kcal/mol.

U5W	CP			UnCP		
	CAM-B3LYP-D3		ω B97XD	CAM-B3LYP-D3		ω B97XD
	6-311+G(d,p)	6-311+G(3d,2p)	aug-cc-pVTZ	6-311+G(d,p)	6-311+G(3d,2p)	aug-cc-pVTZ
U11334	-59.5 (0.0)	-49.3 (0.0)	-48.4 (0.0)	-62.6 (0.0)	-50.7 (0.0)	-54.2 (0.0)
U11224	-58.4 (1.0)	-48.1 (1.1)	-47.8 (0.6)	-61.5 (1.1)	-49.7 (1.1)	-53.0 (1.1)
U12234 anti	-57.9 (1.5)	-48.0 (1.3)	-47.1 (1.3)	-61.0 (1.6)	-49.4 (1.3)	-52.3 (1.9)
U12234 syn	-57.4 (2.1)	-47.9 (1.4)	-46.8 (1.6)	-60.4 (2.1)	-49.3 (1.2)	-52.0 (2.2)
MAE ^a				12.3	0.8	3.8
MAE ^b				3.1	1.5	7.1

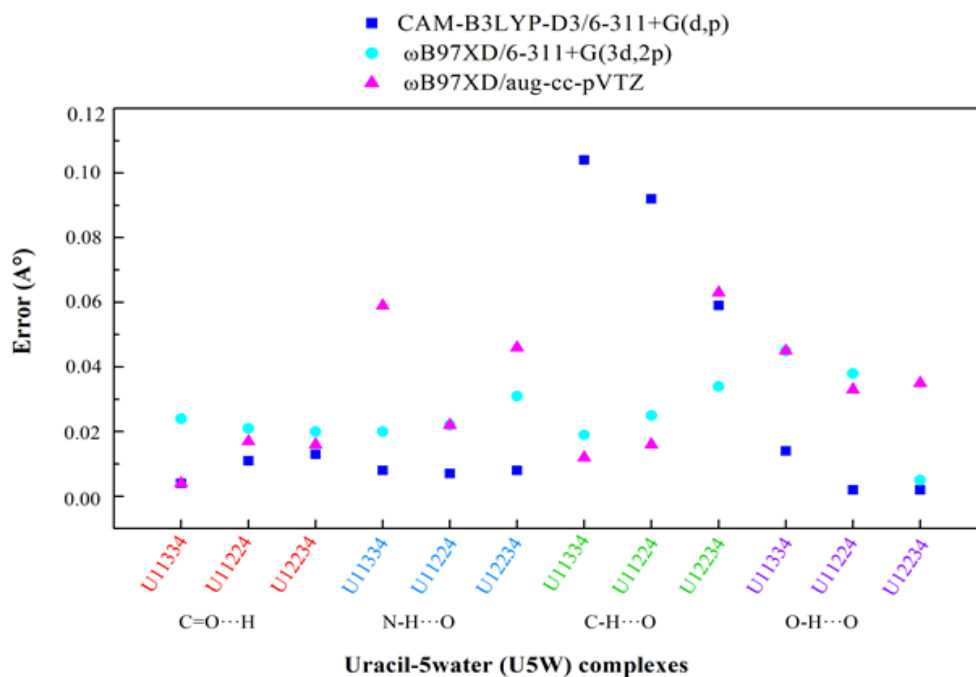


Figure 3. Errors in H-bond lengths (in Å) compared to the B3LYP/DZP++ reference [17]

Regarding H-bond lengths, CAM-B3LYP-D3/6-311+G(d,p) displays negligible deviations for

C=O...H, N-H...O, and O-H...O bonds compared to B3LYP/DZP++ [17], except for the C-H...O

Asma Hennouni, Mohammed El Amine Benmalti, Claude Pouchan, and Panagiotis Karamanis

bond, where the error ranges from 0.1 Å to 0.06 Å, as illustrated in Figure 3. While ω B97XD/6-311+G(3d,2p) and ω B97XD/aug-cc-pVTZ give lower error. In addition, contrary to expectations, the ω B97XD/6-311+G(3d,2p) method exhibits slight errors, estimated at 0.02 Å for the C=O \cdots H, N-H \cdots O, and C-H \cdots O H-bonds, and 0.04 Å for the O-H \cdots O H-bond in both U11334 and U11224 isomers. The consistency between CAM-B3LYP-D3/6-311+G(d,p), ω B97XD/6-311+G(3d,2p), and ω B97XD/aug-cc-pVTZ is demonstrated, particularly in the C=O \cdots H H-bond. It is noteworthy that the differences are most evident in the least stable complex, U12234.

MAE^a of each method (UnCP) compared those at B3LYP/DZP++ [17].

MAE^b difference between BSSE (CP) method and without it (UnCP).

To enhance the clarity and interpretation of the data, we have incorporated Figure 4, which illustrates the interaction energy (ΔE_{int}) with and without CP. The results indicate that CAM-B3LYP-D3/6-311+G(d,p) exhibits a small divergence, with a lower MAE (3.1 kcal/mol) as noted in table 1 compared to the ω B97XD/aug-cc-pVTZ method,

which shows significant divergence with a higher MAE of 7.1 kcal/mol.

This discrepancy arises from the influence of higher-quality basis sets, which naturally reduce BSSE. The inclusion of diffuse functions and improved basis sets further minimizes BSSE, whereas a large BSSE correction suggests an overestimation of UnCP, rendering the ω B97XD/aug-cc-pVTZ method less reliable.

While, the ω B97XD/6-311+G(3d,2p) method demonstrates grand convergence, as evidenced by its negligible MAE, specifically 1.5 kcal/mol as shown in Table 1, and 1.2 kcal/mol for the new complexes in Table 2. Given the high computational cost of BSSE correction, its application is not necessary in this case. This method is considered reliable, as a small BSSE indicates that the basis set is sufficiently large to accurately describe the interaction without introducing excessive artificial stabilization.

The ω B97XD/6-311+G(3d,2p) exhibits lower BSSE than other levels, indicating greater self-consistency and reduced dependence on artificial basis set effects, unlike ω B97XD/aug-cc-pVTZ, which is more influenced by basis set limitations.

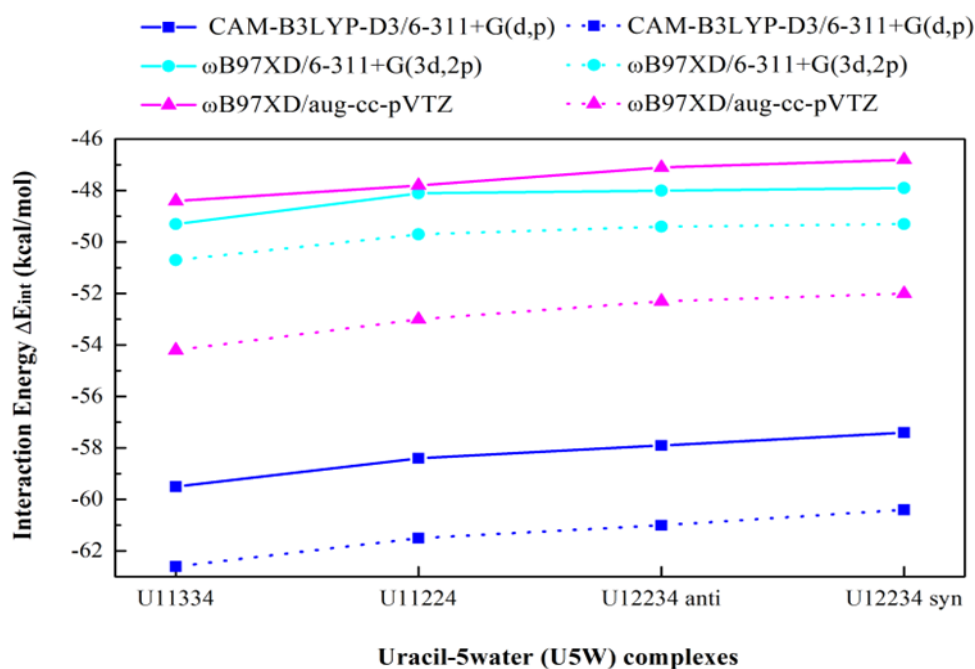


Figure 4. Comparison of CP (solid line) and UnCP (dotted line) calculations for the ΔE_{int} stability of U5W complexes

Asma Hennouni, Mohammed El Amine Benmalti, Claude Pouchan, and Panagiotis Karamanis

Table 2. The interaction energy (ΔE_{int}) and relative interaction energy ΔE_{intrel} in parentheses with both CP and UnCP of new isomers of U5W complexes calculated at the ω B97XD/6-311+G(3d,2p) level theory, expressed in kcal/mol.

U5W	CP		UnCP	
	ΔE_{int}	ΔE_{intrel}	ΔE_{int}	ΔE_{intrel}
U11333	-	-	-53.175	(0.000)
U11133	-52.004	(0.000)	-53.127	(0.048)
New isomers				
U12223	-	-	-52.226	(0.949)
U13333	-	-	-49.911	(3.264)
U11134	-48.624	(3.380)	-49.903	(3.272)
U11123	-48.397	(3.607)	-49.551	(3.624)
U11144	-48.236	(3.768)	-49.252	(3.923)
U11124	-47.233	(4.771)	-48.522	(4.653)
U22244	-46.112	(5.892)	-47.153	(6.022)
U33344	-	-	-46.617	(6.558)
MAE			1.2	

The interaction energies (ΔE_{int}) and relative interaction energies (ΔE_{intrel}) of the U11333 and U11133 isomers, as previously reported by Bachrach et al. [44], and the new identified isomers are reported in Table 2 calculated without (UnCP) and with (CP) basis set superposition error (BSSE) correction.

The new isomer U12223 is the most stable, with an energy of -52.226 kcal/mol. The U11333 isomer is identified as the most stable, displaying the lowest ΔE_{intrel} . This stability is due to the shortest average N-Hu...Ow H-bond length of approximately 1.772 Å, compared to 1.780 Å for U11133 and 1.818 Å for U12223. These findings are consistent with a recent study by [21] where the B3LYP-D/6-311+G(d,p) method is used. However, at the B3LYP/6-311+G(d,p) level [21], the U11333 isomer is less stable than U11223, while at the PBE1PBE/6-311+G(d,p) level [44], it is less stable than U11133, based on the comparison of $\Delta E_{0\text{rel}}$ values with zero-point vibrational energy (ZPVE) corrections. These discrepancies highlight the varying effects of dispersion corrections, with the best agreement observed between the B3LYP-D/6-311+G(d,p) results [19] and our ω B97XD/6-311+G(3d,2p) calculations, similar to what is observed in U3W complexes. The second most stable structure, U11133, exhibits the shortest average H-bond lengths of 1.770 Å (C=Ou...Hw), 1.780 Å (N-Hu...Ow), and 1.754 Å (O-Hw...Ow). The most stable isomers: U11333, U11133,

U12223, and U13333 are characterized by the clustering of three water molecules in a specific region around uracil. These findings confirm the stability of the MMT-derived structure, in which water molecules preferentially aggregate on one side of the uracil plane, consistent with the observations of Danilov et al. [60].

At the ω B97XD/6-311+G(3d,2p) level, a new set of U5W complexes was generated, as illustrated in Figure 5. While the structural inspiration was drawn from previous studies, the present configurations are original and feature systematic placement of water molecules around the four primary binding sites of uracil. Various orientations (syn, anti) and spatial arrangements were considered to thoroughly explore H-bonding patterns and to identify new stable complexes. This approach also served to evaluate the reliability of the computational methodology. The newly identified complexes (Figure 5), were compared with systems listed in Table 1. The U11334, U11224, and U12234 isomers exhibit C-H...O H-bond lengths of 2.500 Å, 2.472 Å, and 2.440 Å, respectively. These results suggest that the newly identified isomers, characterized by their shorter C-H...O H-bonds, are energetically more favorable than the previously analyzed configurations.

In contrast, the corresponding bond lengths in U11134, U11144, and U11124 were found to be 2.482 Å, 2.198 Å, and 2.463 Å, respectively. These results suggest that the newly identified isomers,

characterized by their shorter C-H...O H-bonds, are energetically more favorable than the previously analyzed configurations of Kim et al. [17].

Although structural differences exist between the complexes investigated in this study and those reported by Bachrach et al. [44], a comparative analysis reveals notable similarities in their computational results. Despite variations in molecular composition, both studies exhibit common features, particularly in the clustering patterns of water molecules.

Among the complexes previously reported by Bachrach et al. [44], the relative binding energies ($\Delta E_{\text{bindrel}}$) of (U22233, U22223), (U11122), (U11333, U11133, U11122), and (U33333) show strong correspondence with those of the newly investigated structures (U12223), (U11134), (U11123, U11124), and (U13333), respectively. While Bachrach et al. [44] identified U11133 as the most stable uracil-water complex, our calculations at the ω B97XD/6-311+G(3d,2p) level indicate that U11333 is the most stable, with an ΔE_{int} of -52.004 kcal/mol (Table 2). This result is in agreement with the findings of Thicoipie et al. [21] and Pouchan et al. [42]. This consistency supports the reliability of the ω B97XD method and highlights its agreement with results obtained using the PBE, B3LYP, and B3LYP-D functionals.

These results suggest that, despite differences in structural motifs, the underlying stabilization mechanisms and water clustering effects remain comparable. This reinforces the robustness of our computational approach and highlights its broader applicability to similar molecular systems.

3.2. Spectroscopic properties

The calculated scaled frequencies of the vibrational modes for the U5W complexes using ω B97XD and CAM-B3LYP-D3 methods compared to experimental results are presented in Table 3. The U11334 and U11133 isomers exhibit medium-intensity asymmetric $\nu(\text{OH}(\text{F}))_{\text{asym}}$ modes at approximately 3974 cm^{-1} . Convergence was observed with the ω B97XD/6-311+G(3d,2p) method, while the U11334 isomer at CAM-B3LYP-D3 level showed an extended shift to 3938 cm^{-1} , similar to the behavior seen in the U1W and U2W complexes. The $\nu(\text{OH}(\text{B}))$ bands are strong at ~ 3717 - 3450 cm^{-1} region. The most intense OH(B) band for the U11334 isomer is observed at 3599

cm^{-1} with ω B97XD/6-311+G(3d,2p) and at 3544 cm^{-1} with CAM-B3LYP-D3/6-311+G(d,p). This confirms the presence of O-Hw2...O=C2u and O-Hw1...Ow2 H-bond interactions. For the U11133 isomer, the strongest O-H(B) band calculated at the ω B97XD/6-311+G(3d,2p) level is observed at 3598 cm^{-1} , attributed to the O-Hw3...O=C2u and O-Hw2...Ow3 H-bond interactions. However, the OH(B) at 3544 cm^{-1} in the U11334 isomer is slightly more intense than of the U11133 isomer. Additionally, the $\nu(\text{N1H}(\text{B}))$ and $\nu(\text{N3H}(\text{B}))$ bands of U11334 isomer appear at 3235 cm^{-1} and 3172 cm^{-1} , respectively, which are lower than those of U11133 isomer at 3262 cm^{-1} and 3223 cm^{-1} as shown in Figure 6.

These results can be explained by the strong interactions of water molecules that cluster on one side of first and binding third sites of uracil, compared to the more dispersed interactions across three separate binding sites, as elucidated by Danilov et al. [60]. In the 3000 - 3800 cm^{-1} region, the MAE and maximum (MAX) of CAM-B3LYP-D3 outperform those of ω B97XD/6-311+G(3d,2p) in U11334 isomer by ~ 11 cm^{-1} . However, in the 500 - 1800 cm^{-1} region, both methods yield nearly identical values. These results align with those obtained for the U11133 isomer and show good agreement with the B3LYP/6-31+G(d,p) method [42], which have indicated that vibrational modes primarily associated with ring movements are less affected by the presence of water molecules compared to coupled modes involving NH vibration. This observation aligns with our findings for the U5W complex, as shown in Table 3. The analysis of microhydrated complexes reveals significant variations in the following modes for the U11334 at the CAM-B3LYP-D3 level compared to isolated uracil. Notable shifts include: $\gamma(\text{C-H})$, (N-H) + $\gamma(\text{H}_2\text{O})$ at 961 cm^{-1} , $\nu(\text{N-C})$, $\delta(\text{C6-H})$, (C5-H) at 1200 cm^{-1} , $\delta(\text{N3-H})$ + $\delta(\text{C-H})$ at 1351 cm^{-1} , and $\delta(\text{ring})$, (N1-H) + $\gamma(\text{H}_2\text{O})$ at 548 cm^{-1} . These modes differ from their counterparts in isolated uracil, which correspond to: $\gamma(\text{C6-H})$ + $\nu(\text{ring})$, $\nu(\text{ring})$ + $\delta(\text{C5-H})$, $\nu(\text{C4-N3})$ + $\delta(\text{N3-H})$, and $\delta(\text{ring})$ + $\delta(\text{C=O})$. In the U12223 isomer, the only notable difference is observed in N3H (B), which appears at 2952 cm^{-1} , distinct from the other isomers. This shift is attributed to the N3H...Ow H-bond, where three water molecules are clustered at uracil's second binding site, leading to a unique

Asma Hennoui, Mohammed El Amine Benmalti, Claude Pouchan, and Panagiotis Karamanis

vibrational behavior. The pronounced shift suggests strong H-bond interactions, confirming the stability of the newly identified complex and validating its successful formation. The results of MAE are comparable to those of the U11333 isomer and the

newly identified U12223 isomer, showing good agreement with those obtained at the B3LYP/6-31+G(d,p) level [42]. Notably, U12223 yields the lowest MAE, indicating better predictive performance compared to other complexes.

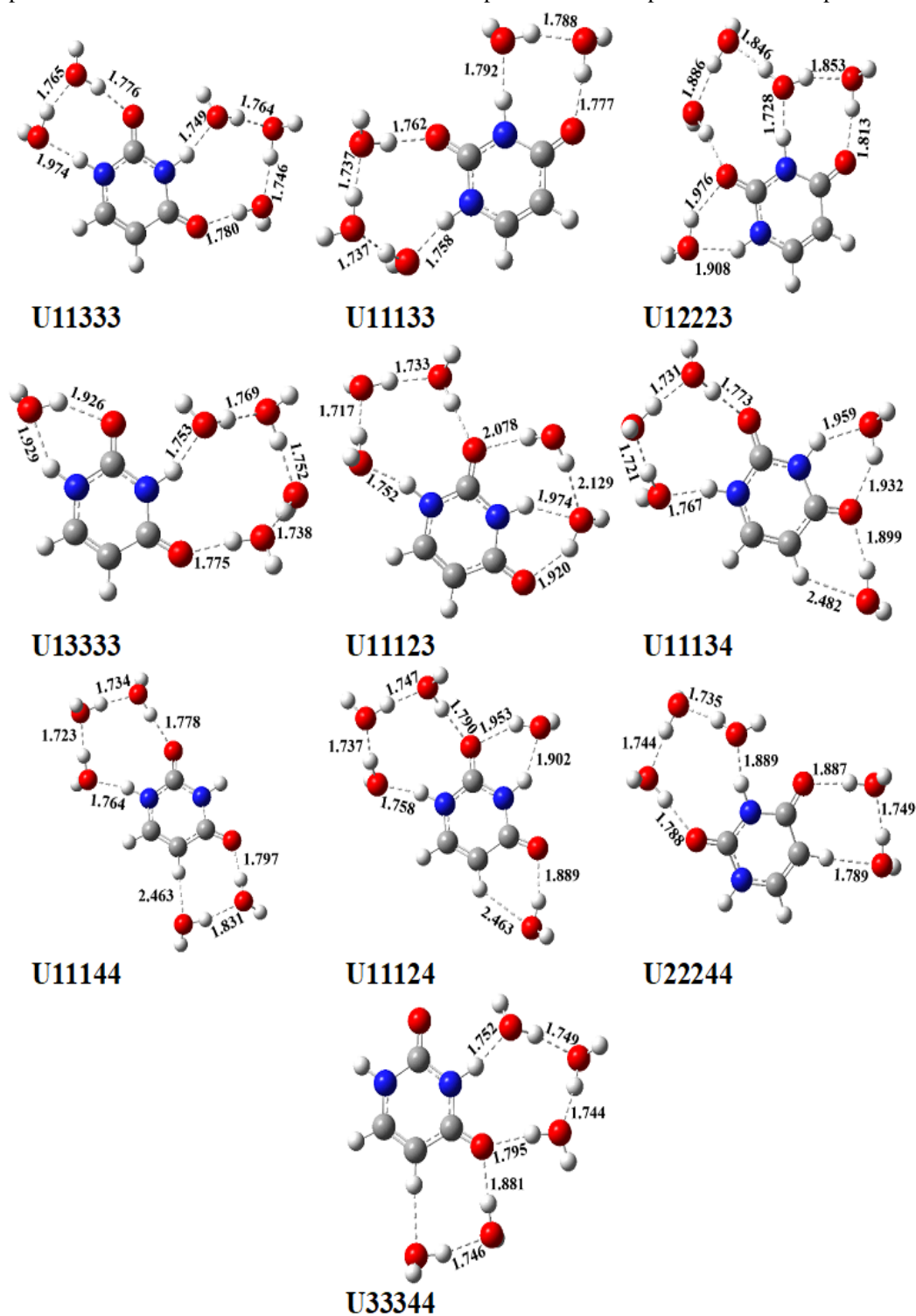


Figure 5. H-bond lengths (in Å) for U11333, U11133, and the new U5W isomers calculated at the ω B97XD/6-311+G(3d,2p) level of theory.

Table 3. Comparison between observed and calculated vibrational wavenumbers in U5W complexes.

assignments	Exp ^a	CAM-B3LYP-D3		ωB97XD				B3LYP ^b			
		6-311+G(d,p)		6-311+G(3d,2p)				6-31+G(d,p)			
		Scaled	Int	Scaled	Int	Scaled	Int	Scaled	Int	VPT2	MD
		U11334	U11334	U11334	U11133	U12223	U5W	U5W	U5W	U5W	U5W
δ(ring) + γ(H ₂ O)	536	511	38	491	86	497	75	535	22	533	529
δ(ring)+γ(H ₂ O)	553	532	193	520	112	519	86	556	23	556	550
δ(ring), (N1-H) + γ(H ₂ O)	573	548	64	546	29	544	12	583	159	568	571
δ(ring) + γ(H ₂ O)	782	738	23	745	9	753	33	751	16	761	775
γ(C-H), (N-H) + γ(H ₂ O)	966	961	2	959	2	971	26	973	6	992	974
δ(ring)+γ(H ₂ O)	1001	1081	1	1077	1	1063	1	1051	1	992	967
ν(N-C), δ(C6-H), (C5-H)	1095	1200	89	1201	87	1194	59	1180	32	1091	1083
δ(C-H) + δ(N-H)	1232	1207	62	1211	64	1206	122	1199	72	1240	1217
δ(N3-H) + δ(C-H)	1387	1351	15	1351	12	1349	15	1386	162	1375	1384
ν(C5=C6) + δ(H ₂ O)	1631	1600	4	1605	43	1615	39	1599	83	1622	1608
ν(C2=O)	1708	1700	850	1704	748	1700	748	1675	979	1684	1654
ν(C6-H), (C5-H) _{asy}	3079	3073	61	3062	9	3068	1258	3067	2	3112	3129
ν(C5-H), (C6-H) _{sym}	3094	3097	6	3108	1026	3104	36	3104	1	3115	3158
3000-3800 cm ⁻¹	MAE	5		16		10		11		-	-
	MAX	6		17		11		12		-	-
500-1800 cm ⁻¹	MAE	37		37		35		26		-	23
	MAX	105		105		99		85		-	-

^a Exp: Observed wavenumbers ref [39,61]

^b Calculated wavenumbers by Pouchan et al [42]

ν : stretching ; δ : in-plane bending ; γ : out-of-plane bending

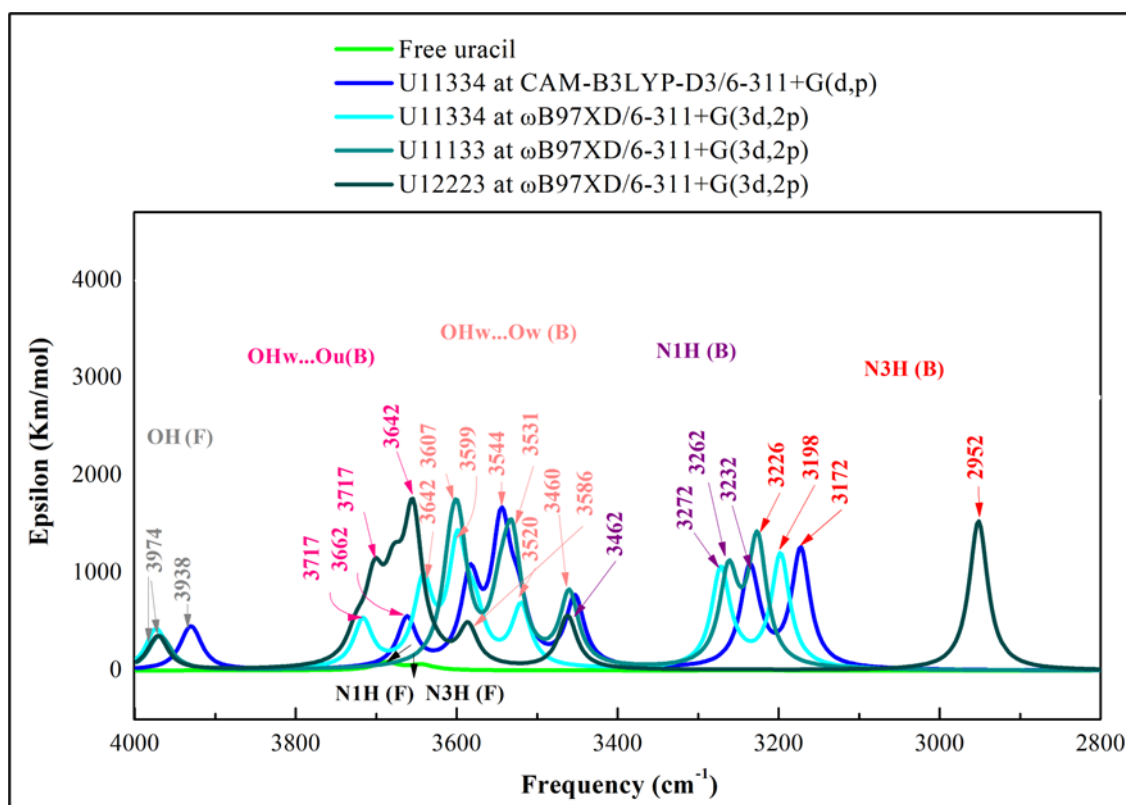


Figure 6. Harmonic vibrational frequencies of ν(OH(F)), ν(OH(B)), ν(N3H(F)), and ν(N1H(B)) in 4000-3200 cm⁻¹ region of U5W complexes

3.3. Solvatochromic shift

The solvatochromic shifts are calculated as the differences in vibrational frequencies between the most stable U5W complexes and isolated uracil, using both harmonic and scaled vibrational frequencies. These shifts are represented in a diagram, where a redshift (negative shift) indicates a decrease in frequency (lower wavenumber), while a blueshift (positive shift) corresponds to an increase in frequency (higher wavenumber).

Figure 7 illustrates the harmonic solvatochromic shifts, whereas Figure 8 displays the scaled vibrational frequencies for selected vibrational modes of the most stable complexes: Specifically, U11334 was analyzed at both the CAM-B3LYP-

D3/6-311+G(d,p) and ω B97XD/6-311+G(3d,2p) levels, while U11333 and the newly identified isomer U12223 were examined at ω B97XD/6-311+G(3d,2p), covering both the functional group and fingerprint regions.

The vibrational modes most affected by the presence of surrounding water molecules are ν (N-H) and ν (C=O) as illustrated in Figure 7. The harmonic modes (7: ν (N1-H)), (6: ν (N3-H)), and (4: ν (C2=O)) exhibit significant redshifts of approximately -200 cm^{-1} , $\sim -400\text{ cm}^{-1}$, and -50 cm^{-1} , respectively, across all isomers.

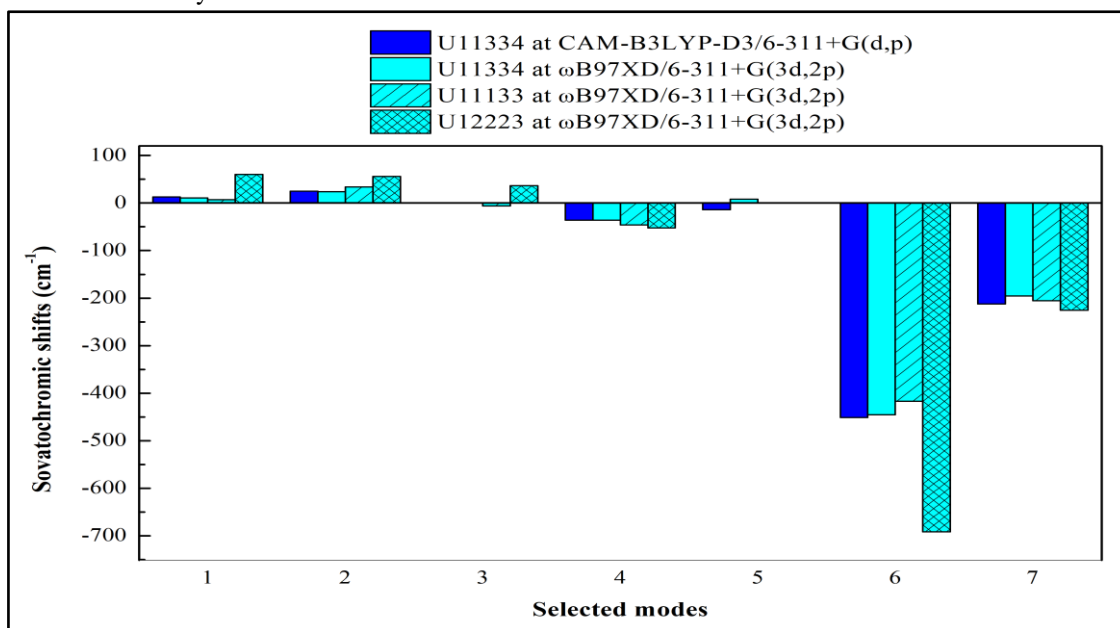


Figure 7. Solvatochromic shifts of harmonic vibrational modes of the most stable complexes. Selected modes: 1: δ [(ring), (N-H)] + γ (H₂O), 2: γ (C-H), δ (N3-H) + γ (H₂O), 3: δ (C-H) + ν (N-C), 4: ν (C2=O), 5: ν [(C5-H), (C6-H)]_{sym}, 6: ν (N3-H), and 7 : ν (N1-H)

These shifts result from H-bond interactions involving N1-Hu \cdots Ow, N3-Hu \cdots Ow, and C2=Ou \cdots Hw.

In contrast, delocalized vibrational modes involving multiple bending modes and OH vibration, such as (1: δ [(ring), (N-H)] + γ (H₂O)) and (2: γ (C-H), δ (N3-H) + γ (H₂O)), exhibit negligible frequency shifts of approximately 12 cm^{-1} and $\sim 25\text{ cm}^{-1}$, respectively, for most isomers, as seen in Figure 7. However, for the newly identified isomer U12223, a more pronounced shift of $\sim 60\text{ cm}^{-1}$ is observed, suggesting enhanced stability comparable to that of the U11333 isomer.

The observed blueshift is attributed to a combination of delocalized mode, bending mode, and weak H-bond. If one part of the vibrational mode strengthens while another weakens, the net effect may favor a blueshift. Additionally, coupling effects can transfer shifts, leading to an overall increase in frequency when a blueshifted bond influences the delocalized mode.

Unlike stretching vibrations, where bond weakening (redshift) or strengthening (blueshift) is directly related to bond length variations, bending modes are more sensitive to molecular rigidity and steric effects. Finally, weak H-bonds are more

electrostatic than covalent-like. In some cases, weak H-bonds induce polarization of the donor bond, making it shorter and stronger, which in turn increases vibrational frequency (blueshift). This effect is observed in modes such as (2: $\gamma(\text{C-H})$, $\delta(\text{N3-H}) + \gamma(\text{H2O})$) and (3: $\delta(\text{C-H}) + \nu(\text{N-C})$) mode. strengthening, which in turn increases the vibrational frequency (blueshift). This effect is observed in modes such as (2: $\gamma(\text{C-H})$, $\delta(\text{N3-H}) + \gamma(\text{H2O})$) and (3: $\delta(\text{C-H}) + \nu(\text{N-C})$). Conversely, strong H-bonds weaken the N-H bond, resulting in significant redshifts, as observed in modes 4, 6, and 7. These findings highlight the contrasting

vibrational behaviors induced by weak and strong H-bonding interactions. Notably, the U12223 isomer exhibits a pronounced redshift (approximately -700 cm^{-1}) in the 6: $\nu(\text{N3-H})$ vibrational mode. This large shift is attributed to the clustering of water molecules around site 2 of the uracil, highlighting the significant role of solvation effects. These observations warrant a broader comparison of vibrational shifts across all isomers, particularly in the 6: $\nu(\text{N3-H})$ and 7: $\nu(\text{N1-H})$ modes. For example, the U11133 isomer, characterized by solvation at site 1, displays a more pronounced redshift in the 7: $\nu(\text{N1-H})$ mode.

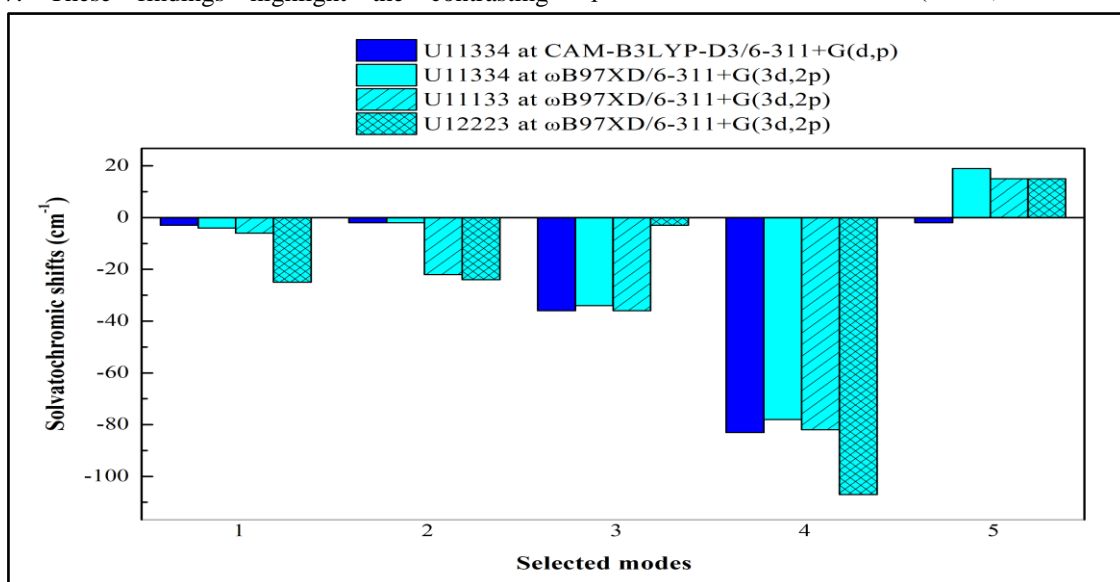


Figure 8. Solvatochromic shifts of scaled vibrational modes of the most stable complexes. Selected modes: 1: $\delta[(\text{ring}), (\text{N-H}) + \gamma(\text{H2O})]$, 2: $\gamma(\text{C-H})$, $\delta(\text{N3-H}) + \gamma(\text{H2O})$, 3: $\delta(\text{C-H}) + \nu(\text{N-C})$, 4: $\nu(\text{C2=O})$, and 5: $\nu[(\text{C5-H}), (\text{C6-H})]_{\text{sym}}$

The delocalized vibrational modes (3: $\delta(\text{C-H}) + \nu(\text{N-C})$) and (5: $\nu[(\text{C5-H}), (\text{C6-H})]_{\text{sym}}$) exhibit negligible redshift for the U11133 isomer and $\sim 25 \text{ cm}^{-1}$ blueshift for U12223, while showing no significant shift for the U11334 isomer. These observations confirm the presence of weak C-H \cdots O H-bonds in U12223. In contrast, mode (5: $\nu[(\text{C5-H}), (\text{C6-H})]_{\text{sym}}$) shows a redshift of $\sim 13 \text{ cm}^{-1}$ exclusively in the U11334 isomer, indicating its involvement in a C5-H \cdots O H-bond, specifically in this complex at the CAM-B3LYP-D3/6-311+G(d,p) level of theory. No significant shift is observed for this mode in the U11133 and U12223 isomers, due to the absence of C-H \cdots O interactions in those complexes.

The scaled vibrational modes corresponding to modes 6 and 7 are not reported due to the absence

of experimental data. As shown in Figure 8, mode (3: $\delta(\text{C-H}) + \nu(\text{N-C})$) undergoes a shift from a minor or negligible shift to a redshift with a solvatochromic shift of $\sim -40 \text{ cm}^{-1}$ in both U11334 and U11133 isomers.

In the U12223 isomer, this mode shifts from a blueshift to a redshift, indicating a change in H-bonding environment or mode coupling.

The harmonic out-of-plane (γ) and in-plane bending (δ) modes, (1: $\delta[(\text{ring}), (\text{N-H})] + \gamma(\text{H2O})$) and (2: $\gamma(\text{C-H})$, $\delta(\text{N3-H}) + \gamma(\text{H2O})$), and (3: $\delta(\text{C-H}) + \nu(\text{N-C})$) display negligible blueshifts for all isomers, as illustrated in Figure 7. However, their scaled modes (Figure 8) reveal a contrasting behavior, resulting in a redshift. Except in U11133 and U12223 which exhibit larger shifts due to their stability compared to U11334 isomer.

The scaling process uniformly adjusts all vibrational modes, but its impact is more pronounced in systems with stronger H-bond interactions and greater structural rigidity. The localized mode (4: $\nu(\text{C}2=\text{O})$) shows significant redshifts compared to harmonic values, indicating that the harmonic vibration tends to underestimate the strength of H-bonding interactions. Additionally, the scaled delocalized mode (5: $\nu[(\text{C}5-\text{H}), (\text{C}6-\text{H})]_{\text{sym}}$) shows no notable variation for the U11334 isomer (Figure 8). This is due to the presence of $\text{C}5-\text{H}\cdots\text{O}$ only at the CAM-B3LYP-D3/6-311+G(d,p) level of theory, whereas the $\omega\text{B}97\text{XD}/6-311+\text{G}(3\text{d},2\text{p})$ method predicts weaker interactions, leading to a blueshift of $\sim 20\text{ cm}^{-1}$. Although there is no H-bonding is present in the U11133 and U12223 isomers, a blueshift is observed after scaling. This suggests that the harmonic calculation may have underestimated the actual bond strength, and the SF correction compensates for this discrepancy, consistent with trends observed in previously discussed modes. Overall, the solvatochromic shift results for U11334 obtained at both CAM-B3LYP-D3/6-311+G(d,p) and $\omega\text{B}97\text{XD}/6-311+\text{G}(3\text{d},2\text{p})$ levels are in close agreement, reinforcing the reliability and consistency of both computational approaches.

4. Conclusions

In this study, we used DFT calculations with dispersion-corrected CAM-B3LYP-D3 and $\omega\text{B}97\text{XD}$ functionals to investigate the microsolvation of uracil through U5W complexes. Energetic, structural, and vibrational properties were analyzed using various basis sets, notably $\omega\text{B}97\text{XD}/6-311+\text{G}(3\text{d},2\text{p})$ and aug-cc-pVTZ, with a focus on newly proposed isomers, particularly U12223. Three highly stable isomers U11334, U11133, and U12223 were identified, where water molecules cluster around key binding sites on uracil. These configurations exhibit strong H-bond interactions, influencing both energetic stability and vibrational properties. The $\omega\text{B}97\text{XD}$ method, especially when corrected for BSSE and combined with the aug-cc-pVTZ basis set, provided results in close agreement with reference data and literature, with U12223 showing the lowest MAE and most reliable predictions. Spectroscopic analysis revealed that solvation significantly impacts $\nu(\text{N}-\text{H})$ and $\nu(\text{C}=\text{O})$ frequencies through redshifts, indicating stronger H-bonding. In contrast, delocalized modes and weak H-bonding interactions were associated with minor blueshifts. The scaling of vibrational frequencies helped

resolve discrepancies in harmonic predictions, particularly for delocalized modes, and confirmed consistent solvatochromic trends across methods. Although CAM-B3LYP-D3 yielded accurate geometries and vibrational profiles, it showed larger deviations in interaction energies compared to $\omega\text{B}97\text{XD}$, likely due to basis set limitations. While CCSD(T) would offer benchmark accuracy for noncovalent interactions, its computational cost was prohibitive for this study. The results obtained in this work can contribute to a deeper understanding of hydration effects on nucleobase analogs and offer improved models for H-bonding in biomolecular systems. Future work will incorporate temperature-dependent dynamics to assess the thermal stability of these complexes.

Acknowledgements

The authors thank the Institut des Sciences Analytiques et de Physico-Chimie pour l'Environnement et les Matériaux (IPREM) for the calculations. We thank Professors Claude Pouchan and Panagiotis Karamanis for their help. Our sincere appreciation goes to Mr. Ali Chahine for his ongoing assistance.

Disclosure Statement: The authors declare that there are no conflicts of interest related to this research.

Funding Information: *This research received no specific grant from any funding agency in the public, commercial, or not-for-profit sectors.*

References

- [1] S. Sivakova, S. J. Rowan, S. J. Rowan, Nucleobases as supramolecular motifs, *Chemical Society Reviews* 34 (2005) 9-21.
- [2] S. Chin, I. Scott, K. Szczepaniak, W. B. Person, Matrix Isolation Studies of Nucleic Acid Constituents. 2. Quantitative ab Initio Prediction of the Infrared Spectrum of In-Plane Modes of Uracil, *Journal of the American Chemical Society* 106 (1984) 3415–3422.
- [3] M. Rozenberg, G. Shoham, I. Reva, R. Fausto, Low temperature Fourier transform infrared spectra and

- hydrogen bonding in polycrystalline uracil and thymine, *Spectrochimica Acta Part A: Molecular and Biomolecular Spectroscopy*, 60 (2004) 2323-2336.
- [4] M. Y. Choi, R. E. Miller, Multiple isomers of uracil-water complexes: Infrared spectroscopy in helium nanodroplets, *Physical Chemistry Chemical Physics* 7 (2005) 3565-3573.
- [5] T. Fornaro, D. Burini, M. Biczysko, V. Barone, Hydrogen-Bonding Effects on Infrared Spectra from Anharmonic Computations: Uracil – Water Complexes and Uracil Dimers, **The Journal of physical chemistry** 119 (2015) 4224-4236.
- [6] V. Barone M. Biczysko, J. Borkowska-Panek, I. Carnimeo, P. Panek, Toward anharmonic computations of vibrational spectra for large molecular systems, *Journal of Quantum Chemistry* 112 (2012) 2185–2200.
- [7] T. Fornaro, M. Biczysko, S. Monti, V. Barone, Dispersion corrected DFT approaches for anharmonic vibrational frequency calculations: nucleobases and their dimers †, *Physical Chemistry Chemical Physics* 16 (2014) 10112–10128.
- [8] T. Fornaro, I. Carnimeo, M. Biczysko, Toward Feasible and Comprehensive Computational Protocol for Simulation of the Spectroscopic Properties of Large Molecular Systems: The Anharmonic Infrared Spectrum of Uracil in the Solid State by the Reduced Dimensionality / Hybrid VPT2 Approach, *The Journal of Physical Chemistry* 119 (2015) 5313-5326.
- [9] T. Fornaro, M. Biczysko, J. Bloino, V. Barone, Reliable vibrational wavenumbers for C Q O and N – H stretchings of isolated and hydrogen-bonded nucleic acid bases †, *Physical Chemistry Chemical Physics* 18 (2016) 8479-8490.
- [10] M. De La Pierre, C. Pouchan, Ab initio periodic modelling of the vibrational spectra of molecular crystals: the case of uracil. *Theoretical Chemistry Accounts* 137 (2018) 25.
- [11] B. Khalili, K. Ghauri, N. Ghavidel, N. Pourhasan, An insight into interaction of the uracil, thymine and cytosine biomolecules with methimazole anti-thyroid drug: DFT and GD3-DFT approaches, *Structural Chemistry* 34 (2023) 1021-1042.
- [12] M. G. Mattioli, L. Avaldi, P. Bolognesi, A. Casavola, F. Morini, T. Van Caekenberghe, P. Rousseau, A study of the valence photoelectron spectrum of uracil and mixed water–uracil clusters, *The Journal of Chemical Physics* 158 (2023) 114301.
- [13] P. Chakraborty, Y. Liu, T. Weinacht, S. Matsika, Effect of dynamic correlation on the ultrafast relaxation of uracil in the gas phase, *Faraday Discussions* 228 (2021) 266-285.
- [14] B. Milovanović, J. Novak, M. Etinski, W. Domcke, N. Došlić, Simulation of UV absorption spectra and relaxation dynamics of uracil and uracil-water clusters, *Chemistry Chemical Physics* 23 (2021) 2594-2604.
- [15] A. Buczek, K. Rzepiela, T. Kupka, M. A. Broda, T. Kar, Uracil-water interaction revisited - in search of single H-bonded secondary minima,

- Physical Chemistry Chemical Physics 26 (2024) 5169-5182.
- [16] L. Biedermannová, B. Schneider, Hydration of proteins and nucleic acids: Advances in experiment and theory. A review, *Biochimica et Biophysica Acta (BBA)-General Subjects* 1860 (2016) 1821-1835.
- [17] S. Kim, H. F. S. Iii, Effects of microsolvation on uracil and its radical anion: Uracil-(H₂O)_n (n= 1–5). *The Journal of chemical physics* 125 (2006) 144305.
- [18] V. B. Delchev, I. G. Shterev, H. Mikosch, Theoretical investigation (DFT and MP2) of the intermolecular proton transfer in the supersystems uracil-(H₂O)_n and uracil-(CH₃OH)_n (n= 1, 2), *Monatshefte für Chemie-Chemical Monthly* 139 (2008) 349-362.
- [19] X. Bao, H. Sun, N. Wong, J. Gu, Microsolvation Effect, Hydrogen-Bonding Pattern, and Electron Affinity of the uracil–water complexes U–(H₂O)_n (n= 1, 2, 3), *The Journal of Physical Chemistry B* 110 (2006) 5865-5874.
- [20] T. Van Mourik, S. L. Price, D. C. Clary, Ab initio calculations on uracil–Water, *The Journal of Physical Chemistry A* 103 (1999) 1611-1618.
- [21] S. Thicoipe, P. Carbonniere, C. Pouchan, The use of the GSAM approach for the structural investigation of low-lying isomers of molecular clusters from density-functional-theory-based potential energy surfaces: The structures of microhydrated nucleic acid bases, *The Journal of Physical Chemistry A* 117 (2013) 7236-7245.
- [22] K. H. Møller, A. S. Hansen, H. G. Kjaergaard, Gas Phase Detection of the NH-P Hydrogen Bond and Importance of Secondary Interactions, *The Journal of Physical Chemistry A* 119 (2015) 10988-10998.
- [23] S. Grimme, J. Antony, S. Ehrlich, H. Krieg, A consistent and accurate ab initio parametrization of density functional dispersion correction (DFT-D) for the 94 elements H-Pu, *The Journal of chemical physics* 132 (2010) 154104.
- [24] M. G. Medvedev, I. S. Bushmarinov, J. Sun, J. P. Perdew, K. A. Lyssenko, Density functional theory is straying from the path toward the exact functional, *Science* 355 (2017) 144305.
- [25] A. J. Cohen, P. Mori-Sánchez, W. Yang, Insights into current limitations of density functional theory, *Science* 321 (2008) 792-794.
- [26] A. F. Rodrigues-Oliveira, F. W. M. Ribeiro, G. Cervi, T. C. Correra, Evaluation of Common Theoretical Methods for Predicting Infrared Multiphotonic Dissociation Vibrational Spectra of Intramolecular Hydrogen-Bonded Ions, *ACS Omega* 3 (2018) 9075-9085.
- [27] D. Grabarek, and T. Andruniów, Assessment of Functionals for TDDFT Calculations of One- and Two-Photon Absorption Properties of Neutral and Anionic Fluorescent Proteins Chromophores, *Journal of Chemical Theory and Computation* 15 (2019) 490–508.
- [28] J. Ree, K. C. Ko, Y. H. Kim, H. K. Shin, Vibrational Energy Flow in the Uracil-H₂O Complexes, *The Journal*

- of Physical Chemistry B 125 (2021) 874-882.
- [29] M. P. Gaigeot, M. Ghomi, Geometrical and vibrational properties of nucleic acid constituents interacting with explicit water molecules as analyzed by density functional theory calculations. 1. Uracil + nwH₂O (nw = 1, ..., 7), The Journal of Physical Chemistry B 105 (2001) 5007-5017.
- [30] R. Bo Zhang, T. Zeegers-Huyskens, A. Ceulemans, M. T. Nguyen, Interaction of triplet uracil and thymine with water, Chemical Physics, 316 (2005) 35-44.
- [31] R. N. Casaes, J. B. Paul, R. P. McLaughlin, R. J. Saykally, T. Van Mourik, Infrared cavity ringdown spectroscopy of jet-cooled nucleotide base clusters and water complexes, The Journal of Physical Chemistry A 108 (2004) 10989-10996.
- [32] M. A. Palafox, N. Iza, M. Gil, The hydration effect on the uracil frequencies: An experimental and quantum chemical study, Journal of Molecular Structure: THEOCHEM 585(2002) 69-92.
- [33] S. Ketkov, E. Rychagova, Electronic excited states of mixed sandwich complexes, (η^7 -C₇H₇) (η^5 -C₅H₅)M (M = V, Cr): Investigation with time-dependent density functional theory, Inorganica Chimica Acta 487 (2018) 281-286.
- [34] M. Juanes, R. T. Saragi, C. Pérez, L. Evangelisti, Enríquez, M. Jaraíz, A. Lesarri, Hydrogen Bonding in the Dimer and Monohydrate of 2-Adamantanol: A Test Case for Dispersion-Corrected Density Functional Methods, Molecules 27 (2022) 2584.
- [35] V. Srinivasadesikan, P. K. Sahu, S. L. Lee, Quantum mechanical calculations for the misincorporation of nucleotides opposite mutagenic 3, N⁴-ethenocytosine, the Journal of Physical Chemistry B 116 (2012) 11173-11179
- [36] K. S. Thanthiriwatte, E. G. Hohenstein, L. A. Burns, C. D. Sherrill, Assessment of the Performance of DFT and DFT-D Methods for Describing Distance Dependence of Hydrogen-Bonded Interactions, Journal of Chemical Theory and Computation 7 (2011) 88-96.
- [37] L. M. da Costa, S. R. Stoyanov, S. Gusarov, X. Tan, M. R. Gray, J. M. Stryker, A. Kovalenko, Density Functional Theory Investigation of the Contributions of π - π Stacking and Hydrogen-Bonding Interactions to the Aggregation of Model Asphaltene Compounds, Energy & Fuels 26 (2012) 2727-2735.
- [38] S. Herbers, P. Kraus, J. U. Grabow, Accurate equilibrium structures of methyl methacrylate and methacrylic acid by microwave spectroscopy and dispersion corrected calculations, The Journal of Chemical Physics 150 (2019) 144308.
- [39] D. Sutradhar, A. K. Chandra, T. Zeegers-Huyskens, Theoretical study of the interaction of fluorinated dimethyl ethers and the ClF and HF molecules. Comparison between halogen and hydrogen bonds, International Journal of Quantum Chemistry 116 (2016) 670-680.
- [40] H. Nouredine, O. Issaoui, N. Medimagh, M. Al-Dossary, O. Marouani, Quantum chemical studies on molecular structure, AIM, ELF, RDG, and antiviral activities of

- hybrid hydroxychloroquine in the treatment of COVID-19: Molecular docking and DFT calculations, *Journal of King Saud University* 33 (2021) 101334.
- [41] T. Tsuzuki, S. Uchamaru, Accuracy of intermolecular interaction energies, particularly those of hetero-atom containing molecules obtained by DFT calculations with Grimme's D2, D3 and D3BJ dispersion corrections, *Physical Chemistry Chemical Physics* 22 (2020) 22508–22519.
- [42] C. Pouchan, S. Thicoipe, M. De La Pierre, DFT modelling of the infrared spectra for the isolated and the micro-hydrated forms of uracil, *Theoretical Chemistry Accounts* 138 (2019) 36.
- [43] A. S. A. Dena, Z. A. Muhammad, W. M. I. Hassan, Spectroscopic, DFT studies, and electronic properties of novel functionalized bis-1,3,4-thiadiazoles, *Chemical Papers* 73 (2019) 1279–1288.
- [44] S. M. Bachrach, M. W. Dzierlenga, Microsolvation of uracil and its conjugate bases: A DFT study of the role of solvation on acidity, *Journal of Physical Chemistry A* 115 (2011) 5674–5683.
- [45] M. J. Frisch, G. W. Trucks, H. B. Schlegel, G. E. Scuseria, M. A. Robb, J. R. Cheeseman, G. Scalmani, V. Barone, G. A. Petersson, H. Nakatsuji, M. Caricato, X. Li, H. P. Hratchian, A. F. Izmaylov, J. Bloino, G. Zheng, J. L. Sonnenberg, M. Hada, M. Ehara, K. Toyota, R. Fukuda, J. Hasegawa, M. Ishida, T. Nakajima, Y. Honda, O. Kiato, H. Nakai, T. Vreven, J. A. Montgomery, J. E. Peralta, F. Ogliaro, M. Bearpark, J. J. Heyd, E. Brothers, K. N. Kudin, V. N. Staroverov, R. Kobayashi, J. Norm, K. Raghavachari, A. Rendell, J. C. Burant, S. S. Iyengar, J. Tomasi, M. Cossi, N. Rega, J. M. Millam, M. J. Klene, E. Knox, J. B. Cross, V. Bakken, C. Adamo, J. Jaramillo, R. Gomperts, R. E. Stratmann, O. Yasyev, A. J. Austin, R. Cammi, C. Pomelli, J. W. Ochterski, R. L. Martin, K. Morokuma, V. G. Zakrzewski, G. A. Voth, P. Salvador, J. J. Dannenberg, S. Dapprich, A. D. Daniels, O. Farkas, J. B. Foresman, J. V. Ortiz, J. Cioslowski, D. J. Fox, Gaussian, Revision A.1, Gaussian Inc., Wallingford, CT (2016).
- [46] F. Samuel Boys, F. Bernardi, The calculation of small molecular interactions by the differences of separate total energies: Some procedures with reduced errors, *Molecular Physics* 19 (1970) 5353–5366.
- [47] R. Wiczorek, L. Haskamp, J. J. Dannenberg, Molecular orbital calculations of water clusters on counterpoise-corrected potential energy surfaces, *J. Phys. Chem. A* 108 (2004) 6713–6723.
- [48] J. Simon, S. M. Silvia, M. Duran, M. Dannenberg, How does basis set superposition error change the potential surfaces for hydrogen-bonded dimers?, *J. Chem. Phys.* 105 (1996) 11024–11031.
- [49] J. Turi, L. Laszlo, J. Dannenberg, Molecular orbital studies of CH...O hydrogen-bonded complexes, *J. Phys. Chem.* 97 (1993) 7899–7909.
- [50] A. D. Becke, Density-functional thermochemistry. V. Systematic optimization of exchange-correlation functionals, *The Journal*

- of Chemical Physics 107 (1997) 8554–8560.
- [51] S. Grimme, Semiempirical hybrid density functional with perturbative second-order correlation, *The Journal of Chemical Physics* 124 (2006) 034108-034108.
- [52] J. Chai, M. Head-gordon, Long-Range Corrected Hybrid Density Functionals with Damped Atom-Atom Dispersion Corrections, *Physical Chemistry Chemical Physics* 10 (2008), 6615-6620.
- [53] S. Grimme, A. Hansen, J. G. Brandenburg, C. Bannwarth, Dispersion-corrected mean-field electronic structure methods, *Chemical Reviews* 116 (2016) 5105–5154.
- [54] T. Yanai, D. P. Tew, N. C. Handy, A new hybrid exchange–correlation functional using the Coulomb-attenuating method (CAM-B3LYP), *Chemical Physics Letters* 393 (2004) 51–57.
- [55] A. D. Becke, Density-functional thermochemistry. III. The role of exact exchange, *The Journal of Chemical Physics* 98 (1993) 5648–5652.
- [56] C. Lee, W. Yang, R. G. Parr, Development of the Colle-Salvetti correlation-energy formula into a functional of the electron density, *Physical Review B* 37 (1988) 785.
- [57] Y. Tawada, T. Tsuneda, S. Yanagisawa, T. Yanai, K. Hirao, A long-range-corrected time-dependent density functional theory, *The Journal of Chemical Physics* 120 (2004) 8425–8433.
- [58] <https://cccbdb.nist.gov/>, May 2022, Accessed :05.01.2025
- [59] <https://www.originlab.com>, OriginPro Version 8.5, Accessed: 24.03.2025.
- [60] V. I. Danilov, T. van Mourik, V. I. Poltev, Modeling of the ‘hydration shell’ of uracil and thymine in small water clusters by DFT and MP2 methods, *Chemical physics letters* 429 (2006) 255–260.
- [61] E. Torres, G. A. DiLabio, A (nearly) universally applicable method for modeling noncovalent interactions using B3LYP, *The Journal of Physical Chemistry Letters* 3 (2012) 1738–1744.